


# Spectral element method with geometric mesh for two-sided fractional differential equations

Zhiping Mao<sup>1</sup> · Jie Shen<sup>2</sup> 

Received: 15 February 2017 / Accepted: 9 August 2017 /  
Published online: 18 August 2017  
© Springer Science+Business Media, LLC 2017

**Abstract** Solutions of two-sided fractional differential equations (FDEs) usually exhibit singularities at the both endpoints, so it can not be well approximated by a usual polynomial based method. Furthermore, the singular behaviors are usually not known *a priori*, making it difficult to construct special spectral methods tailored for given singularities. We construct a spectral element approximation with geometric mesh, describe its efficient implementation, and derive corresponding error estimates. We also present ample numerical examples to validate our error analysis.

**Keywords** Two-sided fractional differential equations · Singularity · Spectral element method · Geometric mesh · Error estimate · Exponential convergence

**Mathematics Subject Classification (2010)** 65N35 · 65E05 · 65M70 · 41A05 · 41A10 · 41A25

---

Communicated by: Martin Stynes

---

✉ Jie Shen  
shen@math.purdue.edu  
Zhiping Mao  
zhiping\_mao@brown.edu

<sup>1</sup> Division of Applied Mathematics, Brown University, 182 George St, Providence RI 02912, USA

<sup>2</sup> Department of Mathematics, Purdue University, West Lafayette, IN 47907-1957, USA

## 1 Introduction

We consider numerical approximation for the two-sided fractional differential equations (FDEs):

$$\begin{aligned} \rho u - p_1 {}_{-1}D_x^\alpha u(x) - p_2 {}_x D_1^\alpha u(x) &= f(x), \quad x \in \Lambda, \\ u(\pm 1) &= 0, \end{aligned} \quad (1.1)$$

where  $1 < \alpha < 2$ ,  $\rho \geq 0$ ,  $p_1, p_2 \geq 0$  and  $p_1 + p_2 \neq 0$ ,  $f(x)$  is a given function,  ${}_{-1}D_x^\alpha u(\cdot)$  and  ${}_x D_1^\alpha u(\cdot)$  are the left-sided and right-sided Riemann-Liouville (R-L) fractional derivative, respectively.

FDEs provides a useful approach to describe transport dynamics in complex systems that are governed by anomalous diffusion and non-exponential relaxation patterns. In addition, the problem (1.1) arises when one discretizes in time parabolic equations with two-sided spatial fractional derivatives, for instance, fractional advection diffusion equations [5, 6, 14, 17, 18], fractional kinetic equation [9], fractional Fokker-Planck equation [22].

It is in general desirable to have high-order numerical methods when solving PDEs, including fractional PDEs. The convergence rate of numerical methods usually depends on the regularity of solutions in suitable functional spaces, e.g., usual Sobolev spaces for polynomial (local or global) based methods. However, it is now well-known that solutions of fractional PDEs usually do not have high regularities in the usual Sobolev spaces. Some high-order methods have been developed for FDEs such as (1.1), e.g., fourth order finite difference schemes [1, 27], spectral methods [13, 15] with the assumption that the solution of FDEs is sufficiently smooth in the usual Sobolev spaces, which does not hold in general.

In some recent work, special treatments have been proposed to deal with the endpoint singularities for FDEs in some special cases of (1.1), such as

- Left-sided FDEs:  $p_1 \neq 0$ ,  $p_2 = 0$ , or Right-sided FDEs:  $p_1 = 0$ ,  $p_2 \neq 0$ ;
- Riesz FDEs:  $p_1 = p_2 \neq 0$ .

For examples, Jin et al. proposed finite element approximations with a regularity reconstruction [11] or regularity pickup [12] to improve the convergence rate for one-sided FDEs; Zayernouri et al. developed in [23, 24] efficient spectral/spectral-element DG methods for a class of one-dimensional FDEs with constant-coefficients and one-sided fractional derivatives by using the so called poly-fractionomials; Chen et al. [3] developed related spectral algorithms and rigorous error analysis using the framework of generalized Jacobi functions in suitably weighted Sobolev spaces, in particular, they showed that the well desired spectral Petrov-Galerkin methods can achieve spectral accuracy even if the solution is not smooth in the usual Sobolev spaces; the authors of this paper [16] extended the analysis and algorithms developed in [3] for one-sided FDEs to Riesz FDEs. However, these results can not be extended to more general FPDEs with two-sided fractional derivatives.

Recently, Zeng et al. [25, 26] developed a generalized spectral collocation method with tunable accuracy for FDEs of variable order with end-point singularities, their

methods enjoy high accuracy if the singular behaviors of the solutions are known *a priori*. However, for general FDEs (1.1), it is in general not possible to determine *a priori* singular behaviors of its solution.

The main purpose of this paper is to develop a spectral-element method (SEM) for the general FDEs with two-sided fractional derivatives (1.1) which can achieve exponential accuracy despite the fact its solution has singularities at the endpoints. The main approach is inspired by the  $h$ - $p$  finite-element method with geometric mesh developed in [8] for second order problems with singular solutions. In particular, for SEM using a geometric mesh with linearly increasing degrees of polynomials in successive subintervals, we develop error estimates in energy norm for both left-sided or two-sided FDEs. Our error estimates show that, for a given geometric mesh with ratio  $q$  combined with a linearly increasing degrees of polynomials, our SEM converges exponentially like  $e^{-C\sqrt{N}}$ , where  $N$  is the total degree of freedom, without the *a priori* knowledge about the singularity. We believe that this is the first time such results are derived for FDEs with general two-sided fractional derivatives.

The rest of this paper is organized as follow: In Section 2, we describe some basic notations and properties for fractional derivatives. We present our SEM and describe the structure of the stiffness matrix in Section 3. Then in Section 4, we carry out an error analysis of the SEM with geometric mesh for both left-sided FDEs and two-sided FDEs. A number of numerical examples are presented to validate our error estimates in Section 5. Some concluding remarks are given in the last section, followed by an appendix where an efficient and stable procedure to evaluate the stiffness matrix is described.

## 2 Preliminaries

We first recall some functional spaces which will be used in this paper.

Let  $\Lambda = (-1, 1)$ , and  $\omega(x) > 0$  ( $x \in \Lambda$ ) be a weight function, we denote by  $L^2_\omega(\Lambda)$  the usual weighted Hilbert space with the inner product and norm defined by

$$(u, v)_{\Lambda, \omega} = \int_{\Lambda} uv \omega dx, \quad \|u\|_{\omega, \Lambda} = (u, u)_{\omega, \Lambda}^{\frac{1}{2}}, \quad \forall u, v \in L^2_\omega(\Lambda). \quad (2.1)$$

We denote by  $H^s_\omega(\Lambda)$  and  $H^s_{0, \omega}(\Lambda)$  (with  $s \geq 0$ ) the usual weighted Sobolev spaces with norm  $\|\cdot\|_{s, \omega, \Lambda}$  and semi-norm  $|\cdot|_{s, \omega, \Lambda}$ . When  $\omega \equiv 1$ , we will drop  $\omega$  from the above notations, and we will also drop  $\Lambda$  and/or  $\Omega$  from the notations if no confusion arises.

Let  $c$  be a generic positive constant independent of any functions and of any discretization parameters. We use the expression  $A \lesssim B$  (respectively  $A \gtrsim B$ ) to mean that  $A \leq cB$  (respectively  $A \geq cB$ ), and use the expression  $A \cong B$  to mean that  $A \lesssim B \lesssim A$ .

We recall now notations and properties of Riemann-Liouville fractional integrals and derivatives [19, 20].

**Definition 1** Let  $s \in [n - 1, n)$  where  $n$  is a given positive integer. The left-sided and right-sided Riemann-Liouville fractional integrals  ${}_a I_x^s$  and  ${}_x I_b^s$  of order  $s$  are defined as

$${}_a I_x^s v(x) := \frac{1}{\Gamma(s)} \int_a^x \frac{v(\tau)}{(x - \tau)^{1-s}} d\tau, \quad \forall x \in [a, b], \tag{2.2}$$

and

$${}_x I_b^s v(x) := \frac{1}{\Gamma(s)} \int_x^b \frac{v(\tau)}{(\tau - x)^{1-s}} d\tau, \quad \forall x \in [a, b], \tag{2.3}$$

respectively, where  $\Gamma(\cdot)$  is the Gamma function.

**Definition 2** Let  $s \in [n - 1, n)$  where  $n$  is a given positive integer. The left-sided and right-sided Riemann-Liouville fractional derivatives  ${}_a D_x^s$  and  ${}_x D_b^s$  of order  $s$  are defined as

$${}_a D_x^s v(x) := \frac{1}{\Gamma(n - s)} \frac{d^n}{dx^n} \int_a^x \frac{v(\tau)}{(x - \tau)^{s-n+1}} d\tau, \quad \forall x \in [a, b], \tag{2.4}$$

and

$${}_x D_b^s v(x) := \frac{(-1)^n}{\Gamma(n - s)} \frac{d^n}{dx^n} \int_x^b \frac{v(\tau)}{(\tau - x)^{s-n+1}} d\tau, \quad \forall x \in [a, b], \tag{2.5}$$

respectively.

It is clear that Riemann-Liouville fractional derivatives are linear operators, i.e.,

$$D^s(\lambda f(x) + \mu g(x)) = \lambda D^s f(x) + \mu D^s g(x) \tag{2.6}$$

where  $D^s$  can be either  ${}_a D_x^s$  or  ${}_x D_b^s$ .

We also recall the following results (cf. [4, 13]) which play important roles in the weak formulation and analysis of FDEs:

**Lemma 1** Let  $1 < s < 2$ , then we have

$$\langle -{}_1 D_x^s w(x), v(x) \rangle_\Lambda = \left( -{}_1 D_x^{\frac{s}{2}} w(x), {}_x D_1^{\frac{s}{2}} v(x) \right)_\Lambda, \quad \forall w, v \in H_0^{\frac{s}{2}}(\Lambda), \tag{2.7}$$

$$\langle {}_x D_1^s w(x), v(x) \rangle_\Lambda = \left( {}_x D_1^{\frac{s}{2}} w(x), -{}_1 D_x^{\frac{s}{2}} v(x) \right)_\Lambda, \quad \forall w, v \in H_0^{\frac{s}{2}}(\Lambda). \tag{2.8}$$

**Lemma 2** Let  $1/2 < s < 1$ , then we have

$$\| -{}_1 D_x^s v(x) \|_{L^2(\Lambda)} \cong \| v(x) \|_{H^s(\Lambda)}, \quad \forall v \in H_0^s(\Lambda), \tag{2.9}$$

$$\| {}_x D_1^s v(x) \|_{L^2(\Lambda)} \cong \| v(x) \|_{H^s(\Lambda)}, \quad \forall v \in H_0^s(\Lambda), \tag{2.10}$$

$$\left( -{}_1 D_x^s v(x), {}_x D_1^s v(x) \right)_\Lambda \cong \| v(x) \|_{H^s(\Lambda)}, \quad \forall v \in H_0^s(\Lambda). \tag{2.11}$$

### 3 Spectral element discretization

We consider in this section a spectral element approximation for two-sided FDEs.

### 3.1 Weak formulation and well-posedness

By virtue of Lemma 1, a weak formulation of problem (1.1) is: Find  $u \in H_0^{\frac{\alpha}{2}}(\Lambda)$ , such that

$$A(u, v) = (f, v), \quad \forall v \in H_0^{\frac{\alpha}{2}}(\Lambda), \quad (3.1)$$

where

$$A(u, v) := \rho(u, v) - p_1 \left( -{}_1D_x^{\frac{\alpha}{2}} u, {}_x D_1^{\frac{\alpha}{2}} v \right) - p_2 \left( {}_x D_1^{\frac{\alpha}{2}} u, -{}_1D_x^{\frac{\alpha}{2}} v \right).$$

The well-posedness of (3.1) has been discussed in [13]. In particular, we immediately obtain from Lemma 2 that,  $A(\cdot, \cdot)$  is continuous and coercive in  $H_0^{\frac{\alpha}{2}} \times H_0^{\frac{\alpha}{2}}$ , i.e.,

$$A(u, v) \lesssim \|u\|_{H^{\alpha/2}} \|v\|_{H^{\alpha/2}}; \quad \|u\|_{H^{\alpha/2}}^2 \lesssim A(u, u), \quad \forall u, v \in H_0^{\frac{\alpha}{2}}(\Lambda).$$

Thanks to the Lax-Milgram lemma, the above problem admits a unique solution  $u \in H_0^{\frac{\alpha}{2}}(\Lambda)$  satisfying

$$\|u\|_{H^{\alpha/2}} \lesssim \|f\|_{(H^{\alpha/2})'}, \quad (3.2)$$

where  $(H^{\alpha/2})'$  is the dual space of  $H^{\alpha/2}$ .

### 3.2 Spectral element approximation

The standard spectral Galerkin method with polynomial basis functions is not suitable for FDEs. For some simple special FDEs, it is possible to obtain better convergence results by choosing special basis functions with built in known singular features of the solution (cf. [3, 16]). However, it is not clear what type of singularities that solutions of general FDEs have, especially for problems with two-sided fractional derivatives. Hence, we adopt a spectral element method (i.e.,  $h$ - $p$  finite element method) with geometric mesh [8] which has proven to be effective to deal with singularities at endpoints.

We split the domain  $\Lambda$  into  $M$  non-overlapping elements:

$$\Lambda_i = (x_{i-1}, x_i), \quad i = 1, 2, \dots, M,$$

Where  $-1 = x_0 < x_1 < \dots < x_M = 1$ . Let  $\mathbb{P}_N$  be the polynomial space whose degree is less than or equal to  $N$ , and define the approximation space

$$X_N = \{v \in C(\Lambda) : v|_{\Lambda_i} \in \mathbb{P}_{n_i}, 1 \leq i \leq M\}, \quad \mathbb{X}_N = \{v \in X_N : v(\pm 1) = 0\}, \quad (3.3)$$

where  $n_i$  is the polynomial degree on the interval  $\Lambda_i$ ,  $i = 1, 2, \dots, M$ , and  $N$  stands for the number of degrees of freedom of  $\mathbb{X}_N$ . We also denote

$$h_i = x_i - x_{i-1}, \quad h = \max_{1 \leq i \leq M} h_i.$$

The spectral element method (SEM) for (3.1) is: Find  $u_N \in \mathbb{X}_N$ , such that

$$A(u_N, v_N) = (I_N f, v_N), \quad \forall v_N \in \mathbb{X}_N, \quad (3.4)$$

where,  $I_N f$  is the interpolation operator in  $X_N$  based on Legendre-Gauss-Lobatto points at all subintervals  $\Lambda_k$ ,  $1 \leq k \leq M$ . The argument for the continuous problem

(3.1) also holds true for spectral element approximation (3.4), i.e., (3.4) admits a unique solution  $u_N \in \mathbb{X}_N$ .

### 3.3 Implementation

We shall use a standard set of basis functions for  $\mathbb{X}_N$ . For the interior unknowns in each subdomain, we use the modal basis  $\{\phi_j^k(x)\}_{0 \leq j \leq n_k-2}^{1 \leq k \leq M}$  for  $\Lambda_k$ ,  $1 \leq k \leq M$ . For  $n_k \geq 2$ ,

$$\phi_j^k(x) = \begin{cases} L_j^k(x) - L_{j+2}^k(x), & x \in \Lambda_k, \\ 0, & \text{else,} \end{cases} \tag{3.5}$$

where  $\{L_j^k(x)\}_{0 \leq j \leq n_k-2}^{1 \leq k \leq M}$  are Legendre polynomials defined on the element  $\Lambda_k$ , and  $n_k$  are the degree of polynomial on  $\Lambda_k$ . For the unknowns at the nodes  $\{x_i\}_{i=1, \dots, M-1}$ , we use the usual hat functions defined as:

$$\hat{h}_k(x) = \begin{cases} \frac{x-x_{k-1}}{x_k-x_{k-1}}, & x \in \Lambda_k, \\ \frac{x_{k+1}-x}{x_{k+1}-x_k}, & x \in \Lambda_{k+1}, \\ 0, & \text{otherwise.} \end{cases} \tag{3.6}$$

It is easy to verify that the above basis functions form a basis for  $\mathbb{X}_N$  with the number of degrees of freedom

$$N = \sum_{i=1}^M n_i - 1.$$

Hence we can write

$$u_N(x) = \sum_{k=1}^M \sum_{j=0}^{n_k-2} u_{kj}^{(1)} \phi_j^k(x) + \sum_{k=1}^{M-1} u_k^{(2)} \hat{h}_k(x). \tag{3.7}$$

Substitute it into (3.4) and let  $v_n$  run through all basis functions of  $\mathbb{X}_N$ , we obtain the linear system:

$$(\rho \mathcal{M} - p_1 S_l^\alpha - p_2 S_r^\alpha)U = F, \tag{3.8}$$

where

$$U = [u_{10}^{(1)}, u_{11}^{(1)}, \dots, u_{1, n_1-2}^{(1)}; \dots; u_{M0}^{(1)}, u_{M1}^{(1)}, \dots, u_{M, n_M-2}^{(1)}; u_1^{(2)}, u_2^{(2)}, \dots, u_{M-1}^{(2)}]^T,$$

$$F = [\tilde{F}, \bar{F}]^T,$$

$$\tilde{F} = [\tilde{f}_{10}, \tilde{f}_{11}, \dots, \tilde{f}_{1, n_1-2}; \dots; \tilde{f}_{M0}, \tilde{f}_{M1}, \dots, \tilde{f}_{M, n_M-2}], \quad \tilde{f}_{kj} = (f, \phi_j^k(x)),$$

$$\bar{F} = [\bar{f}_1, \bar{f}_2, \dots, \bar{f}_{M-1}], \quad \bar{f}_j = (f, \hat{h}_j(x)),$$

$\mathcal{M}$  is the mass matrix, and  $S_l^\alpha, S_r^\alpha$  are corresponding left and right (fractional) stiffness matrices. One can verify that:

$$S_l^\alpha = (S_r^\alpha)^T. \tag{3.9}$$

Hence, we only have to describe how to compute elements of  $S_l^\alpha$ .

Due to the non-local property of fractional derivative, the left fractional stiffness matrix can be written in block form as follows:

$$S = \begin{pmatrix} S_{11} & & & & & \bar{S}_1 \\ S_{12} & S_{22} & & & & \bar{S}_2 \\ S_{13} & S_{23} & S_{33} & & & \bar{S}_3 \\ \vdots & \vdots & \vdots & \ddots & & \vdots \\ S_{1,M-1} & S_{2,M-1} & S_{3,M-1} & \cdots & S_{M-1,M-1} & \bar{S}_{M-1} \\ \tilde{S}_{1,M} & \tilde{S}_{2,M} & \tilde{S}_{3,M} & \cdots & \tilde{S}_{M-1,M} & \tilde{S}_M \\ \hat{S}_1 & \hat{S}_2 & \hat{S}_3 & \cdots & \hat{S}_{M-1} & \hat{S} \end{pmatrix} \quad (3.10)$$

where

$$\begin{aligned} (S_{pq})_{ij} &= (-_1D_x^{\frac{\alpha}{2}} \phi_j^p(x), {}_x D_1^{\frac{\alpha}{2}} \phi_i^q(x)), \quad 1 \leq p \leq q \leq M, \quad 0 \leq i \leq n_q - 2, \quad 0 \leq j \leq n_p - 2; \\ (\bar{S}_k)_{ij} &= (-_1D_x^{\frac{\alpha}{2}} \hat{h}_j(x), {}_x D_1^{\frac{\alpha}{2}} \phi_i^k(x)), \quad 1 \leq k \leq M, \quad 1 \leq j \leq M - 1, \quad 0 \leq i \leq n_k - 2; \\ (\tilde{S}_k)_{ij} &= (-_1D_x^{\frac{\alpha}{2}} \phi_j^k(x), {}_x D_1^{\frac{\alpha}{2}} \hat{h}_i(x)), \quad 1 \leq k \leq M, \quad 1 \leq i \leq M - 1, \quad 0 \leq j \leq n_k - 2; \\ (\hat{S})_{ij} &= (-_1D_x^{\frac{\alpha}{2}} \hat{h}_j(x), {}_x D_1^{\frac{\alpha}{2}} \hat{h}_i(x)), \quad 1 \leq i \leq M - 1, \quad 1 \leq j \leq M - 1. \end{aligned} \quad (3.11)$$

are corresponding modal-modal, nodal-modal, modal-nodal, nodal-nodal block stiffness matrices. Note that, for  $p > q$ , by the definition of basis functions, we know that there is no interaction between  ${}_1D_x^{\frac{\alpha}{2}} \phi_j^p(x)$ ,  $0 \leq j \leq n_p - 2$  and  ${}_x D_1^{\frac{\alpha}{2}} \phi_i^q(x)$ ,  $0 \leq i \leq n_q - 2$ , so all the elements of  $S_{pq}$ ,  $p > q$  are zero.

The computation of mass matrix is standard. Due to the non-local features of fractional derivatives, it is non-trivial to compute efficiently the stiffness matrices associated with the spectral-element formulation. Details for the computation of left fractional stiffness matrix  $S_{pq}^{\alpha}$  is presented in Appendix A.

#### 4 SEM with geometric meshes and their error analysis

We present in this section the SEM with geometric meshes for FDEs and carry out its error analysis. The procedure of the proof follows closely to the original proof given in [8] for regular PDEs. The main difference between [8] and our work is that the error in the  $H^1$  norm is analyzed for regular PDEs in [8], while the error analysis in the fractional Sobolev space  $H^{\alpha/2}$  norm is carried out in our work for fractional PDEs. Although the arguments we use below are quite similar to those used in [8], we believe that this is the first time such estimates are derived for fractional PDEs, and thus it should be verified and documented. More importantly, the analysis for the fractional PDEs clearly shows how the value of fractional order  $\alpha$  affects the convergence, and it also provide guidance on how to choose the optimal ratio  $q$  and the slope  $s$  for a given value of fractional order  $\alpha$ .

### 4.1 SEM with geometric mesh for left-sided FDEs

We first consider the left-sided FDEs ( $p_2 = 0$ ): Find  $u_N \in \mathbb{X}_N$ , such that

$$\rho(u_N, v_N) - p_1(-_1D_x^{\frac{\alpha}{2}} u_N, {}_x D_1^{\frac{\alpha}{2}} v_N) = (f, v_N), \quad \forall v_N \in \mathbb{X}_N. \tag{4.1}$$

In this case, the solution is usually singular at the left boundary. Without loss of generality, we assume that the solution behaves like:

$$u(x) = a(1+x)^\mu + h.o.t., \tag{4.2}$$

where *h.o.t.* denotes terms which are more regular than  $O((1+x)^\mu)$  but also satisfy  $u(-1) = 0$ , in particular, *h.o.t.* denotes terms which are at least order of  $O((1+x)^\nu)$  with  $\nu > \mu$ .

#### 4.1.1 Error estimate

Let  $u(x)$  and  $u_N(x)$  be the solutions of (3.1) with  $p_2 = 0$  and (4.1), respectively. Setting

$$e(x) = u(x) - u_N(x), \tag{4.3}$$

we are interested in an error estimate in the energy norm,

$$\|e\|_E := \|e\|_{\frac{\alpha}{2}} \cong \|_{-1}D_x^{\frac{\alpha}{2}} e\|_{L^2}. \tag{4.4}$$

The second equivalence of the above equation follows from Lemma 2. Next we shall derive approximation errors on each interval  $I = (a, b)$  by the polynomial space  $P_p(I)$ . We shall use the following equivalent notations:

$$\|e\|_{E(I)} \equiv E_p(I) \equiv E_p[a, b].$$

Using (4.2) and the definition of fractional derivative, we have

$$_{-1}D_x^{\frac{\alpha}{2}} u = \frac{a\Gamma(\mu+1)}{\Gamma(\mu+1-\alpha/2)}(1+x)^{\mu-\alpha/2} + h.o.t.,$$

here *h.o.t.* denotes terms which are not only more regular than  $O((1+x)^{\mu-\alpha/2})$  but also satisfy  $u(-1) = 0$ . The second equivalence of (4.4) indicates that the approximation of the solution  $u(x)$  in the energy norm is equivalent to the  $L^2$ -approximation of the fractional derivative of  $u(x)$  of order  $\frac{\alpha}{2}$ , i.e., the  $L^2$ -approximation of  $\frac{a\Gamma(\mu+1)}{\Gamma(\mu+1-\alpha/2)}(1+x)^{\mu-\alpha/2} + h.o.t.$ . Then it follows from [7, Theorem 5 and 7] that we have the following useful lemma by neglecting the high order term (see also [8, Theorem 1.1]):

**Lemma 3** *Let  $E_{n_i}(\Lambda_i)$  be the local error of the spectral element solution of the model problem (4.1) with analytic solution (4.2), and denote*

$$r_i = \frac{\sqrt{x_i+1} - \sqrt{x_{i-1}+1}}{\sqrt{x_i+1} + \sqrt{x_{i-1}+1}}, \quad i = 1, \dots, M.$$



Then

$$E_{n_1}(\Lambda_1) \approx \frac{h_1^{\mu-\frac{\alpha}{2}+\frac{1}{2}}}{n_1^{2\mu-\alpha+1}}. \tag{4.5}$$

Furthermore, if  $0 < r_i^2 < 1 - \frac{1}{n_i}$ ,  $i \geq 2$ , then

$$E_{n_i}(\Lambda_i) \approx \frac{h_i^{\mu-\frac{\alpha}{2}+\frac{1}{2}} r_i^{n_i+\frac{\alpha}{2}-\mu}}{\sqrt{1-r_i^2} n_i^{\mu+1-\frac{\alpha}{2}}} \left( \frac{1}{n_i^{\mu-\frac{\alpha}{2}+\frac{1}{2}}} + (1-r_i^2)^{\mu-\frac{\alpha}{2}+\frac{1}{2}} \right), \tag{4.6}$$

and if  $1 - \frac{1}{n_i} < r_i^2 < 1$ ,  $i \geq 2$ , then

$$E_{n_i}(\Lambda_i) \approx h_i^{\mu-\frac{\alpha}{2}+\frac{1}{2}} \frac{r_i^{n_i+\frac{\alpha}{2}-\mu}}{n_i^{\mu+\frac{1}{2}-\frac{\alpha}{2}}} \left( \frac{1}{n_i^{\mu-\frac{\alpha}{2}+\frac{1}{2}}} + (1-r_i^2)^{\mu-\frac{\alpha}{2}+\frac{1}{2}} \right). \tag{4.7}$$

In the inequalities (4.5)–(4.6), the symbol  $\approx$  means that the ratio of the left and the right hand side is bounded above and below by positive constants which merely depend on  $\mu$ .

*Remark 1* If  $r_i$  is not close to 1, then (4.6) may be written as

$$E_{n_i}(\Lambda_i) \approx h_i^{\mu-\frac{\alpha}{2}+\frac{1}{2}} \left( \frac{1-r_i^2}{2r_i} \right)^{\mu-\frac{\alpha}{2}} \frac{r_i^{n_i}}{n_i^{\mu+1-\frac{\alpha}{2}}}. \tag{4.8}$$

Now we consider the case when a geometric mesh is adopted. By this we mean

$$x_i = -1 + 2q^{M-i}, \tag{4.9}$$

where  $0 < q < 1$ . In this case, we have  $r_i = \frac{1-\sqrt{q}}{1+\sqrt{q}} \equiv r$  for all  $i$ . The geometric mesh (4.9) for  $q = 0.5$ ,  $M = 10$  is showed in Fig. 1.

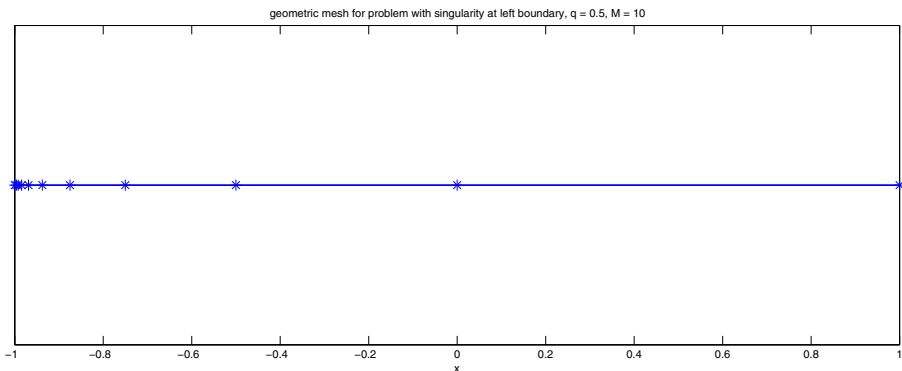


**Fig. 1** Geometric mesh (4.9) for  $q = 0.5$ ,  $M = 10$

Next, we shall try to characterize an optimal degree distribution which minimizes the error (4.4). Let  $\underline{n} = (n_1, n_2, \dots, n_M)$  where  $n_i$  is the polynomial degree in  $\Lambda_i$ . Then by Remark 1, we have

$$\begin{aligned}
 2^{-2(\mu - \frac{\alpha}{2} + \frac{1}{2})} \|e\|_E^2 &\approx \left[ \frac{q^{(M-1)(\mu - \frac{\alpha}{2} + \frac{1}{2})}}{n_1^{2\mu - \alpha + 1}} \right]^2 \\
 &+ \left( \frac{1-r^2}{2r} \right)^{2(\mu - \frac{\alpha}{2})} \sum_{i=2}^M \left[ \frac{(q^{M-i} - q^{M-i+1})^{\mu - \frac{\alpha}{2} + \frac{1}{2}}}{n_i^{\mu + 1 - \frac{\alpha}{2}}} r^{n_i} \right]^2 \\
 &= q^{2(M-1)(\mu - \frac{\alpha}{2} + \frac{1}{2})} \left\{ \frac{1}{n_1^{4\mu - 2\alpha + 2}} \right. \\
 &\quad \left. + \left( \frac{1}{2} \left( \frac{1}{r} - r \right) \right)^{2\mu - \alpha} \sum_{i=2}^M \frac{q^{(2\mu - \alpha + 1)(1-i)}}{n_i^{2\mu + 2 - \alpha}} r^{2n_i} (1-q)^{2\mu - \alpha + 1} \right\} \\
 &= q^{2(M-1)(\mu - \frac{\alpha}{2} + \frac{1}{2})} \left\{ \frac{1}{n_1^{4\mu - 2\alpha + 2}} \right. \\
 &\quad \left. + \left( \frac{1}{2} \left( \frac{1 + \sqrt{q}}{1 - \sqrt{q}} - \frac{1 - \sqrt{q}}{1 + \sqrt{q}} \right) \right)^{2\mu - \alpha} (1-q)^{2\mu - \alpha + 1} \sum_{i=2}^M \frac{q^{(2\mu - \alpha + 1)(1-i)}}{n_i^{2\mu + 2 - \alpha}} r^{2n_i} \right\} \\
 &\approx q^{2(M-1)(\mu - \frac{\alpha}{2} + \frac{1}{2})} \left\{ \frac{1}{n_1^{4\mu - 2\alpha + 2}} \right. \\
 &\quad \left. + q^{\mu - \frac{\alpha}{2}} (1-q) \sum_{i=2}^M \frac{q^{(2\mu - \alpha + 1)(1-i)}}{n_i^{2\mu + 2 - \alpha}} r^{2n_i} \right\}.
 \end{aligned}$$

Denote

$$\mathcal{E}(M, \underline{n}) = \frac{1}{n_1^{4\mu - 2\alpha + 2}} + q^{\mu - \frac{\alpha}{2}} (1-q) \sum_{i=2}^M \frac{q^{(2\mu - \alpha + 1)(1-i)}}{n_i^{2\mu + 2 - \alpha}} r^{2n_i}. \tag{4.10}$$

Then

$$\|e\|_E \approx \eta(M, \underline{n}) \equiv q^{(M-1)(\mu - \frac{\alpha}{2} + \frac{1}{2})} \sqrt{\mathcal{E}(M, \underline{n})}. \tag{4.11}$$

Obviously, for each  $N \geq 2$ , there is  $M \geq 2$  and a degree vector  $\underline{n}^{(M)} = \{n_i^{(M)}\}_{i=1}^M$

with  $\sum_{i=1}^M n_i^{(M)} = N$  such that

$$\eta(M, \underline{n}^{(M)}) = \min \left\{ \eta(k, \underline{n}) \mid 2 \leq k \leq N, \sum_{i=1}^M n_i = N, n_i \geq 1 \right\}.$$

Now let us take a look at the structure of  $\underline{n}^{(M)}$  as  $N \rightarrow \infty$ . We denote

$$D_M = \{ \underline{n} \in \mathbf{R}^M \mid n_i > 0, i = 1, 2, \dots, M \},$$

and for  $N \geq M$ ,

$$D'_{M,N} = \left\{ \underline{n} \in D_M \mid \sum_{i=1}^M n_i = N \right\}.$$

For each  $N \geq 2$ , consider the minimization problem: Find  $(M_N, \underline{n}^{(M_N)})$  with  $\underline{n}^{(M_N)} \in D'_{M,N}$  such that:

$$\eta(M_N, \underline{n}^{(M_N)}) = \min\{\eta(k, \underline{n}) \mid 2 \leq k \leq N, \underline{n} \in D'_{M,N}\}.$$

Since for each  $M$ ,  $D'_{M,N}$  is a connected open set of an  $(M - 1)$ -dimensional hyperplane of  $\mathbf{R}^M$ , and

$$\begin{aligned} \eta(M, \underline{n}) &\geq 0, \quad \forall \underline{n} \in D'_{M,N}, \\ \eta(M, \underline{n}) &\rightarrow \infty, \quad \text{as } \underline{n} \rightarrow \underline{n}_0 \in \partial D'_{M,N}. \end{aligned}$$

It follows that for each  $2 \leq M \leq N$ , one can find a minimizer  $\underline{n}^{(M_N)}$  of  $\eta(M, \cdot)$ . To this end, consider the following Lagrange function with Lagrange multiplier  $\lambda_N$ :

$$\mathcal{L}(\mathcal{E}(M, \underline{n}), \lambda_N) := \mathcal{E}(M, \underline{n}) + 2\lambda_N \left( \sum_{i=1}^M n_i - N \right). \tag{4.12}$$

The the minimizer  $\underline{n}^{(M_N)}$  necessarily satisfies the following conditions:

$$\frac{\partial \mathcal{L}(\mathcal{E}(M, \underline{n}^{(M_N)}), \lambda_N)}{\partial n_1} = \frac{-4\mu + 2\alpha - 2}{(n_1^{(M_N)})^{4\mu - 2\alpha + 3}} + 2\lambda_N = 0, \tag{4.13}$$

$$\begin{aligned} \frac{\partial \mathcal{L}(\mathcal{E}(M, \underline{n}^{(M_N)}), \lambda_N)}{\partial n_i} &= 2Cq^{-(2\mu - \alpha + 1)i} \frac{r^{2n_i^{(M_N)}} (n_i^{(M_N)} \ln r - (\mu + 1 - \frac{\alpha}{2}))}{(n_i^{(M_N)})^{2\mu - \alpha + 3}} \\ &+ 2\lambda_N = 0, \end{aligned} \tag{4.14}$$

where  $C = (1 - q)r^{3\mu - \frac{3\alpha}{2} + 1}$ . Then we can find  $\underline{n}^{(M_N)}$  which minimizes the error.

We will call the sequence  $\{\underline{n}^{(M_N)}\}_{N=2}^\infty$  the sequence of the optimal degree distribution. Clearly, the integer degree distribution  $\underline{n}^{(N)}$  which satisfies  $n_i^N \geq 1$  and  $|n_i^N - n_i^{(M_N)}| < 1$  will give a good rate of convergence.

The next result characterizes the optimal degree distribution asymptotically. An analogous result in the case of regular PDEs is given in [8, Theorem 3.1].

**Theorem 1** *As  $N \rightarrow \infty$ , the asymptotic optimal degree distribution satisfies*

$$\lim_{N \rightarrow \infty} [n_{M_N - i}^{(M_N)} - n_{M_N - i - 1}^{(M_N)}] = s_0, \quad i = 1, 2, \dots, M,$$

with

$$s_0 = \left( \mu + \frac{1}{2} - \frac{\alpha}{2} \right) \frac{\ln q}{\ln r}. \tag{4.15}$$

*Proof* First we notice that as  $N \rightarrow \infty$ , it is possible to obtain a rate of convergence  $e^{-C\sqrt{N}}$  for each  $C > 0$ . This will be proven in Theorem 2. From the expression of  $\eta(M, \underline{n})$ , it is easy to see that if  $M_N$  or  $\max_{1 \leq i \leq M_N} p_i^{(M_N)}$  is bounded by some number,

then we cannot achieve a rate of convergence better than  $N^{-\sigma}$  for some  $\sigma > 0$ . Therefore, for the optimal degree distribution we must have

$$M_N \rightarrow \infty \quad \text{and} \quad \max_{1 \leq i \leq M_N} n_i^{(M_N)} \rightarrow \infty \quad \text{as } N \rightarrow \infty.$$

In fact, we can obtain an even stronger conclusion that for each  $i = 1, 2, \dots$  fixed:

$$n_{M_N-i}^{(M_N)} \rightarrow \infty \quad (\text{as } N \rightarrow \infty)$$

which follows from

$$\eta(M, \underline{n}) > \sqrt{C} \frac{q^{(i-2)(\mu - \frac{\alpha}{2} + \frac{1}{2})} r^{2n_{M_N-i}^{(M_N)}}}{(n_{M_N-i}^{(M_N)})^{2\mu}}.$$

By (4.14) one has that for each  $N \geq 2, i = 2, 3, \dots, M_N$

$$Cq^{-(2\mu-\alpha+1)i} \frac{r^{2n_i^{(M_N)}} \left( n_i^{(M_N)} \ln \frac{1}{r} + (\mu + 1 - \frac{\alpha}{2}) \right)}{(n_i^{(M_N)})^{2\mu-\alpha+3}} = \lambda_N.$$

Let  $n_N(x), 0 < x < \infty$  be the function implicitly defined by the equation

$$Cq^{-(2\mu-\alpha+1)x} \frac{r^{2n_N(x)} \left( n_N(x) \ln \frac{1}{r} + (\mu + 1 - \frac{\alpha}{2}) \right)}{(n_N(x))^{2\mu-\alpha+3}} = \lambda_N. \tag{4.16}$$

Consider the range of the function

$$g(y) = A \frac{r^{2y} \left( y \ln \frac{1}{r} + (\mu + 1 - \frac{\alpha}{2}) \right)}{y^{2\mu-\alpha+3}} \tag{4.17}$$

for any  $A > 0$ . Since  $\lim_{y \rightarrow 0^+} g(y) = +\infty, \lim_{y \rightarrow \infty} g(y) = 0, g : (0, \infty) \rightarrow (0, \infty)$  is onto. Thus for any  $\lambda_N > 0, (4.16)$  is solvable. Use the derivative rule of implicit function to (4.16) we find:

$$\begin{aligned} & \left\{ (n_N(x))^{2\mu-\alpha+3} \left[ q^{(\alpha-2\mu-1)x} (\alpha - 2\mu - 1) \ln q \left( r^{2n_N(x)} \left( n_N(x) \ln \frac{1}{r} + (\mu + 1 - \frac{\alpha}{2}) \right) \right) \right. \right. \\ & + q^{(\alpha-2\mu-1)x} \left( r^{2n_N(x)} 2n'_N(x) \ln r \left( n_N(x) \ln \frac{1}{r} + (\mu + 1 - \frac{\alpha}{2}) \right) + r^{2n_N(x)} \ln \frac{1}{r} n'_N(x) \right) \left. \right. \\ & \left. \left. - q^{(\alpha-2\mu-1)x} r^{2n_N(x)} \left( n_N(x) \ln \frac{1}{r} + \mu + 1 - \frac{\alpha}{2} \right) (2\mu - \alpha + 3) (n_N(x))^{2\mu-\alpha+2} n'_N(x) \right\} \right. \\ & \left. \times \frac{1}{(n_N(x))^{4\mu-2\alpha+6}} = 0 \right. \tag{4.18} \end{aligned}$$

which gives

$$\begin{aligned} n_N(x) & \left[ (\alpha - 2\mu - 1) \ln q \left( n_N(x) \ln \frac{1}{r} + (\mu + 1 - \frac{\alpha}{2}) \right) \right. \\ & \left. + 2n'_N(x) \ln r \left( n_N(x) \ln \frac{1}{r} + (\mu + 1 - \frac{\alpha}{2}) \right) + \ln \frac{1}{r} n'_N(x) \right] \\ & - (2\mu - \alpha + 3) \left( n_N(x) \ln \frac{1}{r} + \mu + 1 - \frac{\alpha}{2} \right) n'_N(x) = 0. \end{aligned} \quad (4.19)$$

After a tedious calculation, we arrive at

$$\begin{aligned} n'_N(x) & = \left( \mu + \frac{1}{2} - \frac{\alpha}{2} \right) \frac{\ln q}{\ln r} \left( 1 - \frac{(\mu - \frac{\alpha}{2} + 1) \left( n_N(x) \ln \frac{1}{r} + (\mu + \frac{3}{2} - \frac{\alpha}{2}) \right)}{n_N(x) \ln r \left( n_N(x) \ln \frac{1}{r} + (\mu + 1 - \frac{\alpha}{2}) \right)} \right)^{-1} \\ & = \left( \mu + \frac{1}{2} - \frac{\alpha}{2} \right) \frac{\ln q}{\ln r} \left( 1 + \frac{(\mu - \frac{\alpha}{2} + 1) \left( n_N(x) \ln \frac{1}{r} + (\mu + \frac{3}{2} - \frac{\alpha}{2}) \right)}{n_N(x) \ln \frac{1}{r} \left( n_N(x) \ln \frac{1}{r} + (\mu + 1 - \frac{\alpha}{2}) \right)} \right)^{-1}. \end{aligned} \quad (4.20)$$

Observe that  $n'_N(x) > 0$ ,  $n_N(i) = n_i^{(M_N)}$  for all  $2 \leq i \leq M_N$ . We obtain that if  $M_N - i - 1 \leq x \leq M_N - i$ , then

$$n_{M_N-i-1}^{(M_N)} \leq n_N(x) \leq n_{M_N-i}^{(M_N)}. \quad (4.21)$$

By mean value theorem

$$n_{M_N-i}^{(M_N)} - n_{M_N-i-1}^{(M_N)} = n'_N(\zeta_{N,i})$$

for some  $M_N - i - 1 \leq \zeta_{N,i} \leq M_N - i$ . For any  $i > 0$  fixed, we have from (4.21) that

$$\lim_{N \rightarrow \infty} n_N(\zeta_{N,i}) = +\infty.$$

It follows from (4.20) that

$$\lim_{N \rightarrow \infty} \left( n_{M_N-i}^{(M_N)} - n_{M_N-i-1}^{(M_N)} \right) = s_0 = \left( \mu + \frac{1}{2} - \frac{\alpha}{2} \right) \frac{\ln q}{\ln r}.$$

□

Now we adopt the geometric mesh (4.9) combining with linear degree vector

$$n_i = \lfloor 1 + s(i - 1) \rfloor, \quad i = 1, 2, \dots, M. \quad (4.22)$$

The value  $s > 0$  will be called the slope. In this case we can let

$$N \approx \frac{sM^2}{2}. \quad (4.23)$$

We then have the following result which is similar to the results obtained in [8, Theorem 3.2].

**Theorem 2** *For the geometric mesh with ratio  $q$  combined with a linear degree vector of slope  $s$ , we have:*

- if  $s > s_0$ , then

$$\|e\|_E \approx C(\mu, q, s) q^{(\mu - \frac{\alpha}{2} + \frac{1}{2})\sqrt{2N/s}}, \quad (4.24)$$

- if  $s < s_0$ , then

$$\|e\|_E \approx C(\mu, q, s)r^{\sqrt{2Ns}}; \tag{4.25}$$

- if  $s = s_0$ , then

$$\|e\|_E \approx C(\mu, q)e^{\sqrt{-(\mu-\frac{\alpha}{2}+\frac{1}{2})N}\sqrt{2\ln q \ln r}}, \tag{4.26}$$

where  $r = \frac{1-\sqrt{q}}{1+\sqrt{q}}$  and  $s_0 = (\mu - \frac{\alpha}{2} + \frac{1}{2})\frac{\ln q}{\ln r}$  is the optimal slope in the sense that the exponential rate attends maximum (with same  $q$ ).

Further more, the optimal geometric mesh and linear degree vector combination is given by

$$q_{op} = (\sqrt{2} - 1)^2, \quad s_{op} = 2\mu - \alpha + 1. \tag{4.27}$$

In this case

$$\|e\|_E \approx C(\mu)[(\sqrt{2} - 1)^2]^{\sqrt{(\mu-\frac{\alpha}{2}+\frac{1}{2})N}}. \tag{4.28}$$

In (4.24)–(4.28), the equivalence constants depends on  $(\mu, q, s)$ ,  $(\mu, q)$  and  $\mu$  respectively.

*Proof* By (4.11), we have

$$\begin{aligned} \|e\|_E &\approx q^{(M-1)(\mu-\frac{\alpha}{2}+\frac{1}{2})} \left\{ 1 + q^{\mu-\frac{\alpha}{2}}(1-q) \sum_{i=2}^M \frac{q^{(2\mu-\alpha+1)(1-i)}r^{2(1+s(i-1))}}{(1+s(i-1))^{2\mu+2-\alpha}} \right\}^{\frac{1}{2}} \\ &= q^{(M-1)(\mu-\frac{\alpha}{2}+\frac{1}{2})} \left\{ 1 + q^{\mu-\frac{\alpha}{2}}(1-q)r^2 \sum_{i=2}^M \frac{e^{(i-1)(2s \ln r - (2\mu-\alpha+1) \ln q)}}{(1+s(i-1))^{2\mu+2-\alpha}} \right\}^{\frac{1}{2}}. \end{aligned} \tag{4.29}$$

If  $2s \ln r - (2\mu - \alpha + 1) \ln q < 0$ , i.e.,

$$s > (\mu - \frac{\alpha}{2} + \frac{1}{2})\frac{\ln q}{\ln r} = s_0,$$

then the sum in the bracket converges as  $M \rightarrow \infty$ , thus

$$\|e\|_E \approx C(\mu, q, s)q^{(M-1)(\mu-\frac{\alpha}{2}+\frac{1}{2})} \approx C(\mu, q, s)q^{(\mu-\frac{\alpha}{2}+\frac{1}{2})\sqrt{2N/s}}. \tag{4.30}$$

If  $s < s_0$ , the quantity in the bracket is of order

$$e^{(M-1)(2s \ln r - (2\mu-\alpha+1) \ln q)} = r^{2s(M-1)}q^{-(M-1)(2\mu-\alpha+1)} \tag{4.31}$$

(as  $M \rightarrow \infty$ ), thus

$$\|e\|_E \approx C(\mu, q, s)r^{s(M-1)} \approx C(\mu, q, s)r^{\sqrt{2Ns}}. \tag{4.32}$$

If  $s = s_0$ , note that  $2\mu + 2 - \alpha > 1$ , so the sum in the bracket also converges, this gives

$$\begin{aligned} \|e\|_E &\approx C(\mu, q)q^{(M-1)(\mu-\frac{\alpha}{2}+\frac{1}{2})} \approx C(\mu, q)q^{(\mu-\frac{\alpha}{2}+\frac{1}{2})\sqrt{2N/s_0}} \\ &\approx C(\mu, q)e^{-\sqrt{(\mu-\frac{\alpha}{2}+\frac{1}{2})N}\sqrt{2\ln q \ln r}}. \end{aligned} \tag{4.33}$$

We now show that  $s = s_0$  gives the best convergence rate and hence it is the optimal slope. As a matter of fact, we have: if  $s > s_0$ , then

$$\begin{aligned} q^{(\mu - \frac{\alpha}{2} + \frac{1}{2})\sqrt{2N/s}} &= e^{(\mu - \frac{\alpha}{2} + \frac{1}{2}) \ln q \sqrt{2N/s}} > e^{(\mu - \frac{\alpha}{2} + \frac{1}{2}) \ln q \sqrt{2N/s_0}} \\ &= e^{-\sqrt{(\mu - \frac{\alpha}{2} + \frac{1}{2})N} \sqrt{2 \ln q \ln r}}; \end{aligned}$$

If  $s < s_0$ , then

$$r^{\sqrt{2Ns}} = e^{\ln r \sqrt{2Ns}} > e^{\ln r \sqrt{2Ns_0}} = e^{-\sqrt{(\mu - \frac{\alpha}{2} + \frac{1}{2})N} \sqrt{2 \ln q \ln r}}.$$

So in either case, the rate of convergence is not better than that when  $s = s_0$ .

At last, by the same argument as in [8, Corollary 3.1], it can be showed that the optimal geometric mesh degree combination is given by

$$q = q_{op} = (\sqrt{2} - 1)^2,$$

and

$$s_{op} = s_0 = \left(\mu - \frac{\alpha}{2} + \frac{1}{2}\right) \frac{\ln q_{op}}{\ln \frac{1 - \sqrt{q_{op}}}{1 + \sqrt{q_{op}}}} = 2\mu - \alpha + 1,$$

thus,

$$\begin{aligned} \|e\|_E &\approx C(\mu) e^{-\sqrt{(\mu - \frac{\alpha}{2} + \frac{1}{2})N} \sqrt{4(\ln(\sqrt{2}-1))^2}} \\ &= C(\mu) [(\sqrt{2} - 1)^2]^{\sqrt{(\mu - \frac{\alpha}{2} + \frac{1}{2})N}}. \end{aligned} \tag{4.34}$$

□

*Remark 2* Theorem 2 shows that, for a given geometric mesh with ratio  $q$  combine with a linear degree vector of slope  $s$ , we can always obtain convergence rate of  $e^{-C\sqrt{N}}$  even if we do not know the singularity behavior at the end point. However, if the leading singularity  $\mu$  is known, then the optimal ratio  $q_{op}$  and slope  $s_{op}$  of the geometric mesh is given in (4.27).

## 4.2 SEM with geometric mesh for two-sided FDEs

For the two-sided fractional PDE (1.1), the solution usually has singularities at both end points for given smooth data. Therefore, in this subsection, we apply the SEM with a different type of geometric mesh to solve Eq. 1.1.

Since the singularities exist at both boundaries, we first split it into two subdomains  $[-1, 0]$  and  $[0, 1]$ , then for given ratios  $0 < q_l, q_r < 1$ , we use the geometric mesh defined as:

$$\begin{aligned} x_i &= -1 + q_l^{\frac{M}{2} - i} \in [-1, 0], \quad i = 1, 2, \dots, \frac{M}{2}, \\ x_i &= 1 - q_r^{i - \frac{M}{2}} \in [0, 1], \quad i = M - 1, M - 2, \dots, \frac{M}{2} + 1, \end{aligned} \tag{4.35}$$

with linear degree vectors as follows:

$$\begin{aligned}
 n_i &= \lfloor 1 + s_l(i - 1) \rfloor, \quad (i = 1, 2, \dots, \frac{M}{2}), \\
 n_i &= \lfloor 1 + s_r(M - i) \rfloor, \quad (i = M - 1, M - 2, \dots, \frac{M}{2} + 1),
 \end{aligned}
 \tag{4.36}$$

where  $s_l$  and  $s_r$  are the absolute values for the slopes of degree vectors to the left and right boundaries, respectively. Here for the sake of simplicity, the number of elements,  $\frac{M}{2}$ , is set to be the same for both subdomains. Figure 2 shows the geometric mesh (4.35) for  $q_l = q_r = 0.5, M = 16$ .

Clearly, the error  $\|e\|_E$  on  $(-1, 1)$  is the sum of the errors of subintervals  $(-1, 0)$  and  $(0, 1)$ , i.e.,

$$\|e\|_E = \|e\|_{E_l} + \|e\|_{E_r},$$

where  $\|e\|_{E_l} := \|e\|_{E([-1,0])}$  and  $\|e\|_{E_r} := \|e\|_{E([0,1])}$ . With the help of Lemma 2, we can write

$$\|e\|_{E_l} = \|_{-1} D_x^{\frac{\alpha}{2}} e \|_{0,[-1,0]} \quad \text{and} \quad \|e\|_{E_r} = \|_x D_1^{\frac{\alpha}{2}} e \|_{0,[0,1]}.$$

In order to obtain estimates for  $\|e\|_{E_l}$  and  $\|e\|_{E_r}$ , we assume that the solution behaves like:

$$u(x) = a(1 + x)^\mu(1 - x)^\nu + h.o.t., \tag{4.37}$$

where *h.o.t.* represents terms more regular than  $(1 + x)^\mu(1 - x)^\nu$  satisfying  $u(\pm 1) = 0$ . Therefore, all the arguments for (4.3) discussed in last subsection also hold true for  $\|e\|_{E_l}$  and  $\|e\|_{E_r}$ . In view of Theorem 2, there are nine possibilities for different values of  $s_l, s_r$  and  $\mu, \nu$ . For the sake of simplicity, we let  $q_l = q_r = q, s_l = s_r = s$ , and  $\mu = \nu$ , so that the total degree of freedom is

$$N \approx sM^2. \tag{4.38}$$

In this case, Theorem 2 leads immediately to the following result:

**Theorem 3** *Let  $u$  be the solution of the two-sided fractional PDE (3.1) and  $u_N$  be the solution of SEM (3.4) with the geometric mesh (4.35) with ratio  $q$  combined with the degree vectors (4.36) of slope  $s$ . Then, we have:*

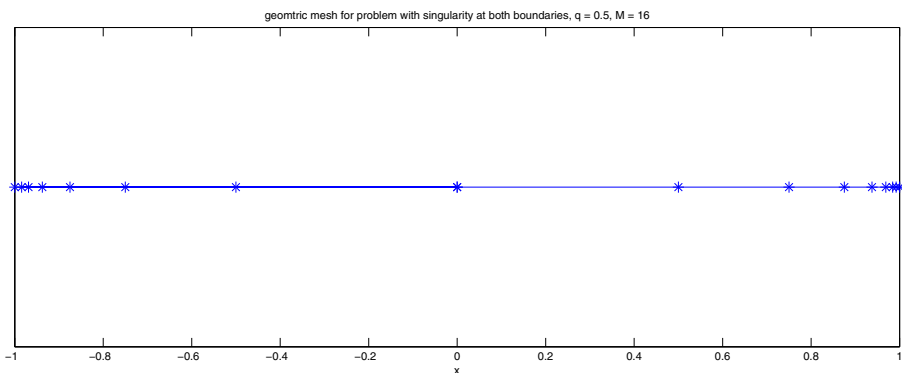


**Fig. 2** Geometric mesh (4.35) for  $q = 0.5, M = 16$



- if  $s > s_0$ , then

$$\|e\|_E \approx \widehat{C}(\mu, q, s)q^{(\mu - \frac{\alpha}{2} + \frac{1}{2})\sqrt{N/s}}; \quad (4.39)$$

- if  $s < s_0$ , then

$$\|e\|_E \approx \widehat{C}(\mu, q, s)r^{\sqrt{Ns}}; \quad (4.40)$$

- if  $s = s_0$ , then

$$\|e\|_E \approx \widehat{C}(\mu, q)e^{\sqrt{-(\mu - \frac{\alpha}{2} + \frac{1}{2})N/2}\sqrt{2\ln q \ln r}}, \quad (4.41)$$

where  $r = \frac{1 - \sqrt{q}}{1 + \sqrt{q}}$  and  $s_0 = (\mu - \frac{\alpha}{2} + \frac{1}{2})\frac{\ln q}{\ln r}$  is the optimal slope (with given  $q$ ).

Similarly, the optimal geometric mesh ratio  $q$  and the slope  $s$  are also given by (4.27). In this case

$$\|e\|_E \approx \widehat{C}(\mu)[(\sqrt{2} - 1)^2]^{\sqrt{(\mu - \frac{\alpha}{2} + \frac{1}{2})N/2}}. \quad (4.42)$$

*Remark 3* As in Remark 2, Theorem 3 indicates that we can always achieve a convergence rate of  $e^{-C\sqrt{N}}$  for a given geometric mesh with ratio  $q$  and a slope  $s$ , and we can choose the optimal  $q$  and  $s$  if  $\mu$  and  $\nu$  are known.

## 5 Numerical tests

We present below several numerical tests to show the effectiveness of the SEM and to verify the error estimates. All figures are plotted in  $\sqrt{N}$  – log scale in order to show a convergence rate of  $e^{-C\sqrt{N}}$ .

We first apply the SEM to left-sided problem (4.1).

*Example 1* Let  $\rho = 1$ , suppose we have a exact solution

$$u(x) = (1 + x) - 2^{1-\gamma}(1 + x)^\gamma, \quad (5.1)$$

where  $\gamma$  is a positive fractional number.

Since the solution contain both a smooth term  $1 + x$  and a non-smooth term  $2^{1-\gamma}(1 + x)^\gamma$ , so neither spectral approximation [15] using Jacobi polynomials nor Petrov-spectral-Galerkin approximation [3] using general Jacobi functions can give good convergence. The exact solution (5.1) only contain singularity at the left endpoint, so we using the spectral element approximation with geometric mesh (4.9) with a linear degree vector (4.22). In the test, we set  $\alpha = 1.2$ ,  $\gamma = 0.6$  or  $\alpha = 1.6$ ,  $\gamma = 0.8$ . Figure 3 shows the convergence in  $L^2$  and  $H^{\frac{\alpha}{2}}$  for the two sets of data. Here the mesh ratio is set to be  $q = (\sqrt{2} - 1)^2$ , corresponding optimal slope  $s = (\gamma - \frac{\alpha}{2} + \frac{1}{2})\frac{\ln q}{\ln r}$ .

We also present the convergence rate in  $H^{\frac{\alpha}{2}}$  in Fig. 4 with different combinations of ratio  $q$  and the corresponding optimal slope  $s$ . The  $H^{\frac{\alpha}{2}}$  convergence results with  $q = (\sqrt{2} - 1)^2$  and different  $s$  are shown in Fig. 5.

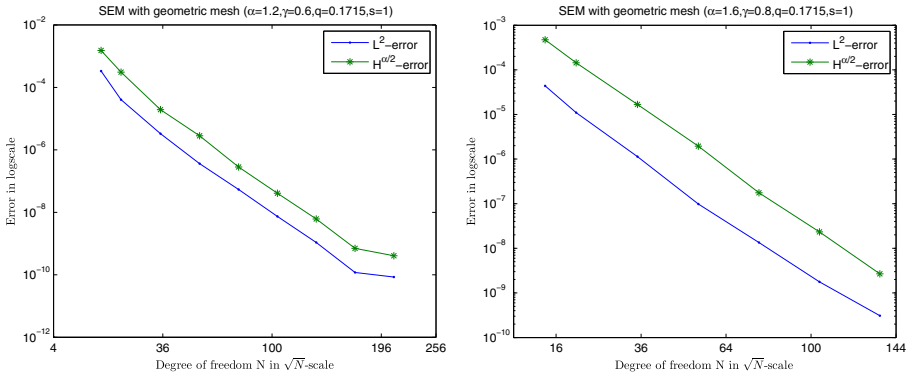


**Fig. 3**  $L^2$  and  $H^{\frac{\alpha}{2}}$  errors of SEM based on geometric mesh for example 1. (left:  $\alpha = 1.2$ ,  $\gamma = 0.6$ , right:  $\alpha = 1.6$ ,  $\gamma = 0.8$ )

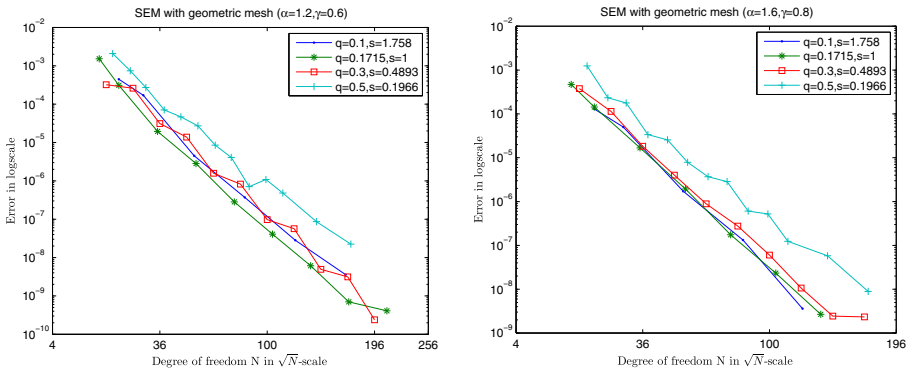


**Fig. 4**  $H^{\frac{\alpha}{2}}$  errors of SEM based on geometric mesh for example 1 with different  $q$  and corresponding optimal  $s$  (left:  $\alpha = 1.2$ ,  $\gamma = 0.6$ , right:  $\alpha = 1.6$ ,  $\gamma = 0.8$ )

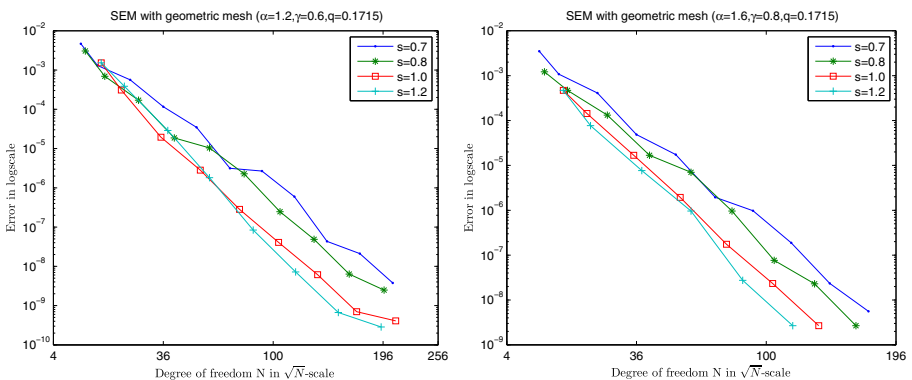


**Fig. 5**  $H^{\frac{\alpha}{2}}$  errors of SEM based on geometric mesh for example 1 with  $q = (\sqrt{2} - 1)^2 \approx 0.1715$  and different  $s$  (left:  $\alpha = 1.2$ ,  $\gamma = 0.6$ , right:  $\alpha = 1.6$ ,  $\gamma = 0.8$ )

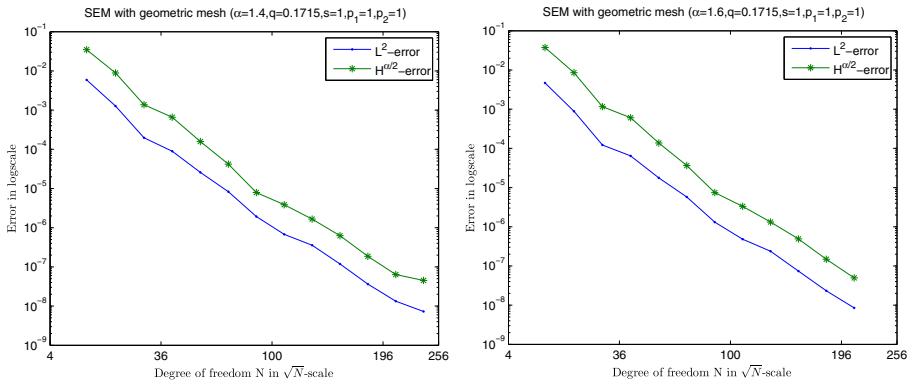


**Fig. 6**  $L^2$  and  $H^{\frac{\alpha}{2}}$  errors with SEM based on geometric mesh for example (2) ( $p_1 = 1, p_2 = 1$ , left:  $\alpha = 1.4$ , right:  $\alpha = 1.6$ )

We observe that the errors in all figures have a convergence rate of  $e^{-C\sqrt{N}}$ , which is in agree with the error estimates (4.24)–(4.26).

Furthermore, Fig. 4 shows that, for different combinations of  $q$  and the corresponding optimal value of  $s$ , the optimal value of  $q = (\sqrt{2} - 1)^2 \approx 0.1715$  with the corresponding optimal slope  $s$  gives the best result. On the other hand, Fig. 5 shows that, for the given optimal value of  $q = (\sqrt{2} - 1)^2$ , the optimal value of  $s = (\gamma - \frac{\alpha}{2} + \frac{1}{2}) \frac{\ln q}{\ln r}$  (or the value very close to it) gives better convergence rate in  $H^{\frac{\alpha}{2}}$ .

In the next example, we solve the two-sided FDEs (1.1) with a smooth right-hand side function  $f$ .

*Example 2* Let  $\rho = 1$  and

$$f(x) = -\cos\left(\frac{\alpha\pi}{2}\right)(2\Gamma(1 + \alpha) + \Gamma(3 + \alpha)x).$$

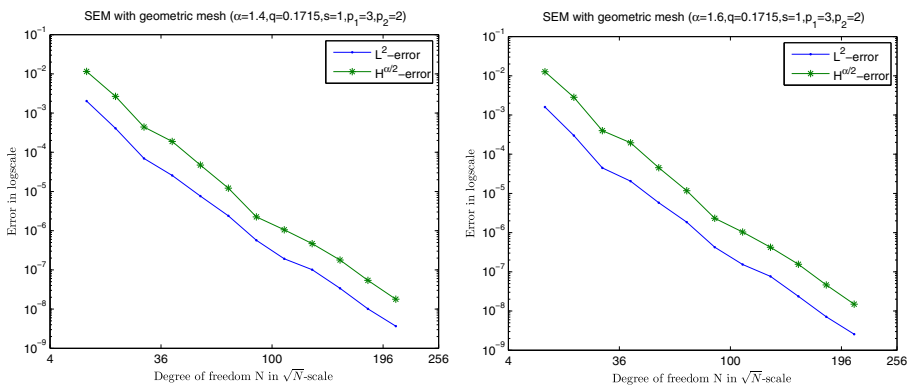


**Fig. 7**  $L^2$  and  $H^{\frac{\alpha}{2}}$  errors with SEM based on geometric mesh for example (2) ( $p_1 = 3, p_2 = 2$ , left:  $\alpha = 1.4$ , right:  $\alpha = 1.6$ )

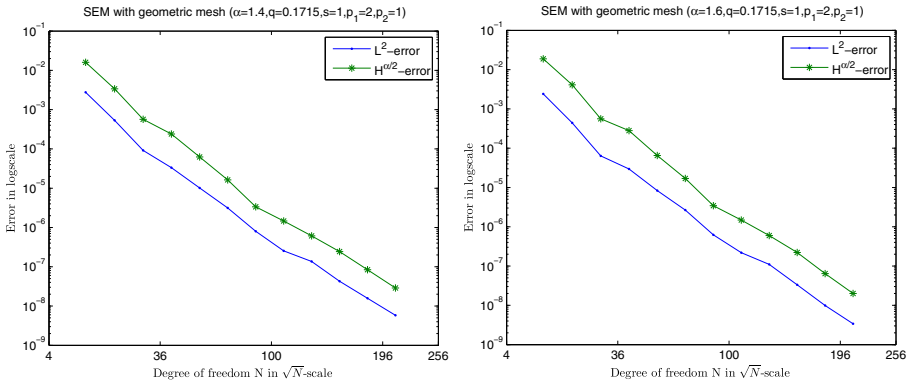


**Fig. 8**  $L^2$  and  $H^{\frac{\alpha}{2}}$  errors with SEM based on geometric mesh for example (2) ( $p_1 = 2, p_2 = 1$ , left:  $\alpha = 1.4$ , right:  $\alpha = 1.6$ )

It is well-known that the solution of (1.1) is singular at  $x = \pm 1$ . We test different values of fractional order  $\alpha$  and different sets of  $(p_1, p_2)$  with optimal value of ratio  $q_l = q_r = q = (\sqrt{2} - 1)^2$ . The value of slope is set to be  $s_l = s_r = s = 1$ . Since no exact solution is available, we use the numerical solution with  $M = 32$  as the reference solution.

Figures 6, 7 and 8 show the convergence rate in  $L^2$  and  $H^{\frac{\alpha}{2}}$  for  $\alpha = 1.4, 1.6$  and  $(p_1, p_2)$  equals to  $(1, 1), (3, 2), (2, 1)$ . Again, we observe that, in all cases, the errors converge like  $e^{-C\sqrt{N}}$ .

Finally, we comment on the conditioning of the linear system (3.8). Let

$$A = \rho \mathcal{M} - p_1 S_l^\alpha - p_2 S_r^\alpha,$$

and set  $q = (\sqrt{2} - 1)^2, s = 1$ , we computed the condition numbers of  $A$  for geometric meshes (4.9) ( $\rho = 1, p_1 = 1, p_2 = 0$ ) and (4.35) ( $\rho = 1, p_1 = 1, p_2 = 1$ )

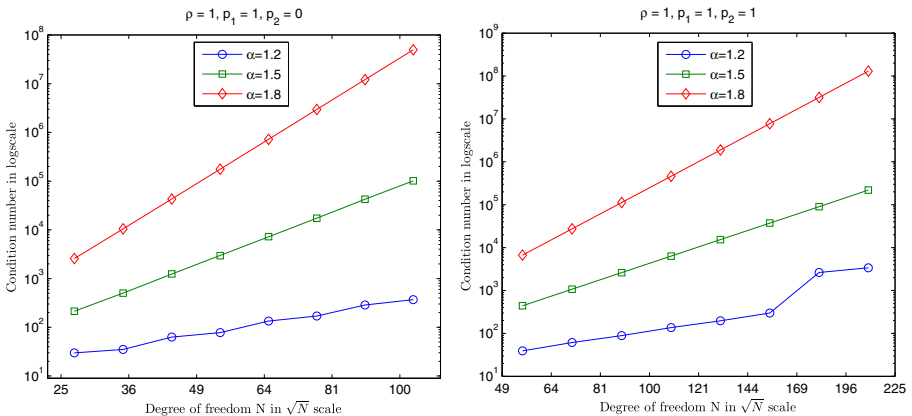


**Fig. 9** Condition number of  $A$  (left: geometric mesh (4.9),  $\rho = 1, p_1 = 1, p_2 = 0$ , right: geometric mesh (4.35),  $\rho = 1, p_1 = 1, p_2 = 1$ )

with linear degree vectors. The results are presented in Fig. 9 (in  $\sqrt{N}$ -log scale). We observe that the condition numbers grow exponentially with respect to  $\sqrt{N}$  for all  $\alpha$ , but larger value of  $\alpha$  leads to faster rate, as expected. For the results presented in this paper, simple Gaussian elimination is used. For larger problems in multi-dimension, it will become necessary to develop efficient preconditioning techniques for the system matrix.

## 6 Concluding remarks

Solutions of fractional diffusion equations with two-sided fractional derivatives usually has singularities at the boundaries, and in general forms of these singularities are unknown and complicated. This makes it hard to design high-order numerical methods which require prior knowledge about the singularities.

Inspired by the success of  $h$ - $p$  finite-element methods with geometric mesh for singular problems, we developed a spectral-element approximation using a geometric mesh with linear degree distribution of polynomials, and derived corresponding error estimates. We showed that, for two-sided fractional diffusion equations with unknown singularities at both ends, the SEM with geometric mesh can achieve exponential convergence rate of  $e^{-C\sqrt{N}}$ , where  $N$  is the total number of unknowns. We also gave specific guidelines on how to choose the geometric mesh ratio  $q$  and the linear degree distribution slope  $s$  in different situations.

Another difficulty involved with the fractional PDEs is that the fractional derivatives are nonlocal operators, making it very expensive to compute stiffness matrices. We developed efficient and stable algorithms to compute the stiffness matrices.

We applied our algorithms to solve the one-sided FDEs as well as two-sided FDEs. Our numerical results indicate that the convergence rate of the proposed SEM with geometric meshes converge like  $e^{-C\sqrt{N}}$  in all situations, without prior knowledge about the singular behaviors at the end points.

**Acknowledgments** Z.M. is supported in part by the MURI/ARO on “Fractional PDEs for Conservation Laws and Beyond: Theory, Numerics and Applications” (W911NF-15-1-0562).

J.S is supported in part by AFOSR FA9550-16-1-0102 and NSF DMS-1620262, and by NSFC grants 11371298, 91630204 and 11421110001.

## Appendix: A Computation of stiffness matrix

We provide below details on how to compute the left fractional stiffness matrix  $S_l^\alpha$ .

The following lemma can be readily verified by Lemma 1 and integration by parts.

**Lemma 4** *Let  $\zeta(x)$ ,  $\eta(x)$  be any two basis functions given by (3.5) or (3.6), then we have*

$$\left(-_1 D_x^{\frac{\alpha}{2}} \zeta(x), {}_x D_1^{\frac{\alpha}{2}} \eta(x)\right) = -\left(-_1 D_x^{\alpha-1} \zeta(x), \eta'(x)\right) = \left(\zeta'(x), {}_x D_1^{\alpha-1} \eta(x)\right) \quad (\text{A.1})$$

First of all, for the nodal-nodal block matrix  $\widehat{S}$ , the explicit formula is given in [10].

### A.1 Modal-modal block matrices

Next, we consider the modal-modal block matrices  $S_{pq}$ ,  $1 \leq p \leq q \leq M$ . Denote  $\phi_j(x) = L_j(x) - L_{j+2}(x)$ . Case I:  $p = q$ .

$$\begin{aligned} (S_{pq})_{ij} &= (-1 D_x^{\frac{\alpha}{2}} \phi_j^p(x), {}_x D_1^{\frac{\alpha}{2}} \phi_i^q(x)) = ({}_{x_{p-1}} D_x^{\frac{\alpha}{2}} \phi_j^p(x), {}_x D_{x_p}^{\frac{\alpha}{2}} \phi_i^q(x))_{\Lambda_p} \\ &= \left(\frac{h_p}{2}\right)^{1-\alpha} (-1 D_x^{\frac{\alpha}{2}} \phi_j(x), {}_x D_1^{\frac{\alpha}{2}} \phi_i(x)), \quad 0 \leq i, j \leq n_q - 2. \end{aligned} \tag{A.2}$$

The last inner product of above equation is the left fractional stiffness matrix for one domain Legendre-Spectral Galerkin method, and can be compute exactly by Legendre-Gauss quadrature. More details can be found in [15].

Let  $n_{max} := \max\{n_i, i = 1, \dots, M\}$ . We observe from (A.2) that we only need to compute the block stiffness matrix with polynomial degree  $n_{max}$ .

Case II:  $p = q - 1$ .

Using (A.1), we have

$$\begin{aligned} (S_{pq})_{ij} &= (-1 D_x^{\frac{\alpha}{2}} \phi_j^p(x), {}_x D_1^{\frac{\alpha}{2}} \phi_i^q(x)) = -({}_x D_x^{\alpha-1} \phi_j^p(x), \frac{d}{dx} \phi_i^q(x)) \\ &= -({}_{x_{p-1}} \mathcal{D}_{x_p}^{\alpha-1} \phi_j^p(x), \frac{d}{dx} \phi_i^q(x))_{\Lambda_q}, \quad 0 \leq i \leq n_q - 2, \quad 0 \leq j \leq n_p - 2, \end{aligned} \tag{A.3}$$

where

$${}_{x_{p-1}} \mathcal{D}_{x_p}^{\alpha-1} \phi_j^p(x) := \frac{1}{\Gamma(2-\alpha)} \int_{x_{p-1}}^{x_p} \frac{d}{ds} \phi_j^p(s) (x-s)^{1-\alpha} ds. \tag{A.4}$$

Note that  ${}_x D_x^{\alpha-1} \phi_j^p(x)$  is different from the point value,  ${}_x D_x^{\alpha-1} \phi_j^p(x)|_{x=x_p}$  denoted by  ${}_{x_{p-1}} D_{x_p}^{\alpha-1} \phi_j^p(x_p)$ .

We present next two methods to compute the inner product in (A.3). The first one is to rewrite it as:

$$\begin{aligned} & -({}_{x_{p-1}} \mathcal{D}_{x_p}^{\alpha-1} \phi_j^p(x), \frac{d}{dx} \phi_i^q(x))_{\Lambda_q} \\ &= -({}_{x_{p-1}} D_x^{\alpha-1} \phi_j^p(x), \frac{d}{dx} \phi_i^q(x))_{\Lambda_q} + ({}_{x_p} D_x^{\alpha-1} \phi_j^p(x), \frac{d}{dx} \phi_i^q(x))_{\Lambda_q}. \end{aligned} \tag{A.5}$$

Then

$$\begin{aligned} & ({}_{x_{p-1}} D_x^{\alpha-1} \phi_j^p(x), \frac{d}{dx} \phi_i^q(x))_{\Lambda_q} \\ &= \frac{1}{\Gamma(2-\alpha)} \int_{-1}^1 \left(\frac{h_{p+1}}{4}(1+t) + \frac{h_p}{2}\right)^{2-\alpha} \frac{d}{dt} \phi_i(t) \int_{-1}^1 (1-\tau)^{1-\alpha} \frac{d}{ds} \phi_j^p(s_{p-1}(\tau)) d\tau dt, \end{aligned} \tag{A.6}$$

where  $s_{p-1}(\tau) = \frac{x-x_{p-1}}{2}\tau + \frac{x+x_{p-1}}{2}$ , and

$$\begin{aligned} & ({}_{x_p} D_x^{\alpha-1} \phi_j^p(x), \frac{d}{dx} \phi_i^q(x))_{\Lambda_q} \\ &= \frac{1}{\Gamma(2-\alpha)} \int_{-1}^1 \left(\frac{h_{p+1}}{4}(1+t)\right)^{2-\alpha} \frac{d}{dt} \phi_i(t) \int_{-1}^1 (1-\tau)^{1-\alpha} \frac{d}{ds} \phi_j^p(s_p(\tau)) d\tau dt, \end{aligned} \tag{A.7}$$

where  $s_p(\tau) = \frac{x-x_p}{2}\tau + \frac{x+x_p}{2}$ .

All these integrals can be computed by Jacobi-Gauss quadrature with suitable Jacobi indices. However, it only work for polynomials of low degree, and becomes computationally unstable for higher degree polynomials which are used in geometric meshes.

Thus, we provide below a less elegant but more stable approach to compute (A.3). Using two transforms:  $x = \frac{h^{p+1}}{2}(1+t) + x_p$  and  $s = \frac{h^p}{2}(1+\tau) + x_{p-1}$ , then by (A.4), we have that Eq. A.3 becomes

$$\begin{aligned} & - (x_{p-1} \mathcal{D}_{x_p}^{\alpha-1} \phi_j^p(x), \frac{d}{dx} \phi_i^q(x))_{\Lambda_q} \\ &= \frac{-1}{\Gamma(2-\alpha)} \left(\frac{h_p}{2}\right)^{1-\alpha} \int_{-1}^1 \frac{d}{dt} \phi_i(t) \int_{-1}^1 \left(1-\tau + \frac{h_{p+1}}{h_p}(1+t)\right)^{1-\alpha} \frac{d}{d\tau} \phi_j(\tau) d\tau dt. \end{aligned} \quad (\text{A.8})$$

Let us first look at the inner integral. Note that  $\frac{d}{d\tau} \phi_j(\tau) = -(2j+3)L_{j+1}(\tau)$  [21]. So the inner integral becomes  $\int_{-1}^1 (x-\tau)^{1-\alpha} L_{j+1}(\tau) d\tau$  (with  $x > 1$ ) which is a special case of

$$\tilde{P}_j^{\alpha,\beta,\nu}(x) := \frac{1}{\Gamma(\nu)} \int_{-1}^1 (x-s)^{\nu-1} P_j^{\alpha,\beta}(s) ds, \quad x > 1. \quad (\text{A.9})$$

The main difficulty in computing the above integral is the singular term  $(x-s)^{\nu-1}$ . We shall compute them by using a hybrid method given in [2, section 3.2] with the main idea being to use three-term recurrence relation for  $x$  near 1, while applying Gauss quadrature for  $x$  away from 1. Then, we can use the Legendre-Gauss quadrature to compute the outer integral.

*Remark 4* Observe that for each entry of the block stiffness matrices, the second method needs to compute the outer integral with a lot of Gauss points to obtain high accuracy due to the weakly singularity ( $x$  near the point  $x_p$ ), so it is very expensive. However, with special mesh, e.g. uniform mesh and geometric mesh, we only need to compute one block matrix. Indeed, for uniform mesh, set  $h_p = h$ ,  $p = 1, 2, \dots, M$ , then (A.8) becomes

$$\frac{-1}{\Gamma(2-\alpha)} \left(\frac{h}{2}\right)^{1-\alpha} \int_{-1}^1 \frac{d}{dt} \phi_i(t) \int_{-1}^1 (2+t-\tau)^{1-\alpha} \frac{d}{d\tau} \phi_j(\tau) d\tau dt. \quad (\text{A.10})$$

For geometric mesh, Let  $x_0 = a$ ,  $x_i = a + (b-a)\eta^{M-i}$ ,  $i = 1, 2, \dots, M$  with  $\eta \in (0, 1)$  is a given constant, (A.5) becomes

$$\frac{-(b-a)^{1-\alpha}}{\Gamma(2-\alpha)} \left(\frac{\eta^{M-m-2}}{2(1-\eta)}\right)^{1-\alpha} \int_{-1}^1 \frac{d}{dt} \phi_i(t) \int_{-1}^1 \left(1 + \frac{1}{\eta}(1+t) - \tau\right)^{1-\alpha} \frac{d}{d\tau} \phi_j(\tau) d\tau dt, \quad (\text{A.11})$$

Observe that the integrals in (A.10) and (A.11) are both independent of  $p$  and  $q$ . Therefore, we only need to compute the block matrix  $S_{pq}$  with either  $n_p = n_{max}$  or  $n_q = n_{max}$ ,  $p = q - 1$ . This also holds true for the first method.

Case III:  $p < q - 1$ .

One can easily obtain that, for  $0 \leq i \leq n_q - 2, 0 \leq j \leq n_p - 2$ ,

$$(S_{pq})_{ij} = \frac{-1}{\Gamma(2 - \alpha)} \int_{-1}^1 \frac{d}{dt} \phi_i(t) \int_{-1}^1 \left( \frac{h_{p+1}}{2}(1+t) - \frac{h_{q+1}}{2}(1+\tau) + x_p - x_q \right)^{1-\alpha} \frac{d}{d\tau} \phi_j(\tau) d\tau dt. \tag{A.12}$$

Since the integrands associated with both fractional derivative and inner product are smooth, they can be computed by the Legendre-Gauss quadrature.

*Remark 5* For uniform mesh or geometric mesh, as discussed in Remark 4, we only need to compute  $M - 2$  block matrixes  $\{S_{pM}\}_{i,j=0}^{n_{max}-2}$  for  $p = 1, \dots, M - 2$ , then any other block matrix  $S_{pq}, p < q - 1$  can be obtained by scaling  $S_{M-q+p+1,M}$ .

### A.2 Nodal-modal and modal-nodal block matrices

Finally, we consider the nodal-modal, modal-nodal block matrices, i.e.  $\bar{S}_k$  and  $\tilde{S}_k, 1 \leq k \leq M$ .

For  $(\bar{S}_k)_{ij}, 1 \leq j \leq M - 1, 0 \leq i \leq n_k - 2$ , with the help of (A.1), we have

$$(\bar{S}_k)_{ij} = -(-1D_x^{\alpha-1} \hat{h}_j(x), \frac{d}{dx} \phi_i^k(x)) = -(-1D_x^{\alpha-1} \hat{h}_j(x), \frac{d}{dx} \phi_i^k(x))_{\Lambda_k}. \tag{A.13}$$

The fractional derivative of  $\hat{h}_j(x)$ , i.e.  $-1D_x^{\alpha-1} \hat{h}_j(x)$ , denoted by  $I_j(x)$ , can be rewritten as:

$$I_j(x) = -1D_x^{\alpha-1} \hat{h}_j(x) = \frac{1}{\Gamma(2 - \alpha)} \int_{-1}^x (x - t)^{1-\alpha} \hat{h}'_j(t) dt,$$

which can be computed exactly:

$$I_j(x) = \begin{cases} 0, & x < x_{j-1}, \\ \frac{h_j^{-1}}{\gamma_\alpha} g(x, x_{j-1}), & x_{j-1} \leq x < x_j, \\ \frac{h_j^{-1}}{\gamma_\alpha} [g(x, x_{j-1}) - g(x, x_j)] - \frac{h_{j+1}^{-1}}{\gamma_\alpha} g(x, x_j), & x_j < x \leq x_{j+1}, \\ \frac{h_j^{-1}}{\gamma_\alpha} [g(x, x_{j-1}) - g(x, x_j)] + \frac{h_{j+1}^{-1}}{\gamma_\alpha} [g(x, x_{j+1}) - g(x, x_j)], & x > x_{j+1}, \end{cases} \tag{A.14}$$

where  $\gamma_\alpha = \Gamma(3 - \alpha)$  and  $g(x, x_j) := (x - x_j)^{2-\alpha}$ . Thus, we can calculate the integral (A.13) by arguing as follows.

- Case I:  $k \leq j - 1$ .

$$(\bar{S}_k)_{ij} = 0. \tag{A.15}$$



- Case II:  $k = j$ .

$$\begin{aligned} (\bar{S}_k)_{ij} &= -\left(I_j(x), \frac{d}{dx}\phi_i^k(x)\right)_{\Lambda_k} = -\frac{h_j^{-1}}{\gamma_\alpha} \int_{x_{j-1}}^{x_j} (x - x_{j-1})^{2-\alpha} \frac{d}{dx}\phi_i^k(x) dx \\ &= -\frac{h_j^{1-\alpha}}{2^{2-\alpha}\gamma_\alpha} \int_{-1}^1 (1+t)^{2-\alpha} \frac{d}{dt}\phi_i(t) dt. \end{aligned} \quad (\text{A.16})$$

Then the integral can be computed by Jacobi-Gauss quadrature with respect to weight  $\omega^{0,2-\alpha}(x)$ .

- Case III:  $k = j + 1$ .

$$\begin{aligned} (\bar{S}_k)_{ij} &= -\left(I_j(x), \frac{d}{dx}\phi_i^k(x)\right)_{\Lambda_k} \\ &= \frac{-h_j^{-1}}{\gamma_\alpha} \int_{x_{j-1}}^{x_j} (x - x_{j-1})^{2-\alpha} \frac{d}{dx}\phi_i^k(x) dx \\ &\quad + \frac{h_j^{-1} + h_{j+1}^{-1}}{\gamma_\alpha} \int_{x_{j-1}}^{x_j} (x - x_j)^{2-\alpha} \frac{d}{dx}\phi_i^k(x) dx \\ &= \frac{-h_j^{-1}}{\gamma_\alpha} \int_{-1}^1 \left(\frac{h_{j+1}}{2}(1+t) + h_j\right)^{2-\alpha} \frac{d}{dt}\phi_i(t) dt \\ &\quad + \left(\frac{h_{j+1}^{-1} + h_j^{-1}}{2^{2-\alpha}\gamma_\alpha} h_{j+1}^{2-\alpha}\right) \int_{-1}^1 (1+t)^{2-\alpha} \frac{d}{dt}\phi_i(t) dt. \end{aligned} \quad (\text{A.17})$$

The first integral can be computed by the Legendre-Gauss quadrature and the second one can be computed by the Jacobi-Gauss quadrature with respect to the weight  $\omega^{0,2-\alpha}(x)$ .

- Case IV:  $k = j + 2$ . Similarly, we have

$$\begin{aligned} (\bar{S}_k)_{ij} &= \frac{-h_j^{-1}}{\gamma_\alpha} \int_{-1}^1 \left(\frac{h_{j+2}}{2}(1+t) + h_j + h_{j+1}\right)^{2-\alpha} \frac{d}{dt}\phi_i(t) dt \\ &\quad + \left(\frac{h_{j+1}^{-1} + h_j^{-1}}{\gamma_\alpha}\right) \int_{-1}^1 \left(\frac{h_{j+2}}{2}(1+t) + h_{j+1}\right)^{2-\alpha} \frac{d}{dt}\phi_i(t) dt \\ &\quad - \frac{h_{j+1}^{-1} h_{j+2}^{2-\alpha}}{2^{2-\alpha}\gamma_\alpha} \int_{-1}^1 (1+t)^{2-\alpha} \frac{d}{dt}\phi_i(t) dt. \end{aligned} \quad (\text{A.18})$$

The first two integrals can be computed by the Legendre-Gauss quadrature and the last one can be computed by the Jacobi-Gauss quadrature with respect to the weight  $\omega^{0,2-\alpha}(x)$ .

- Case V:  $k > j + 2$ .

$$\begin{aligned}
 (\bar{S}_k)_{ij} &= \frac{-h_j^{-1}}{\gamma_\alpha} \int_{-1}^1 \left( \frac{h_k}{2}(1+t) + x_{k-1} - x_{j-1} \right)^{2-\alpha} \frac{d}{dt} \phi_i(t) dt \\
 &\quad + \left( \frac{h_{j+1}^{-1} + h_j^{-1}}{\gamma_\alpha} \right) \int_{-1}^1 \left( \frac{h_k}{2}(1+t) + x_{k-1} - x_j \right)^{2-\alpha} \frac{d}{dt} \phi_i(t) dt \\
 &\quad - \frac{h_{j+1}^{-1}}{\gamma_\alpha} \int_{-1}^1 \left( \frac{h_k}{2}(1+t) + x_{k-1} - x_{j+1} \right)^{2-\alpha} \frac{d}{dt} \phi_i(t) dt.
 \end{aligned} \tag{A.19}$$

All three integrals above can be computed by the Legendre-Gauss quadrature.

Finally, for  $\tilde{S}_k$ ,  $1 \leq k \leq M$ , by using (A.1), we have

$$(\tilde{S}_k)_{ij} = \left( \frac{d}{dx} \phi_j^k(x), {}_x D_1^{\alpha-1} \hat{h}_i(x) \right) = \left( \frac{d}{dx} \phi_j^k(x), {}_x D_1^{\alpha-1} \hat{h}_i(x) \right)_{\Lambda_k}. \tag{A.20}$$

Then we can apply the same argument as for  $\bar{S}_k$  to compute  $\tilde{S}_k$ .

## References

1. Chen, M., Deng, W.: Fourth order accurate scheme for the space fractional diffusion equations. *SIAM J. Numer. Anal.* **52**(3), 1418–1438 (2014)
2. Chen, F., Xu, Q., Hesthaven, J.S.: A multi-domain spectral method for time-fractional differential equations. *J. Comput. Phys.* **293**, 157–172 (2015)
3. Chen, S., Shen, J., Wang, L.-L.: Generalized Jacobi functions and their applications to fractional differential equations. *Math. Comp.* **85**(300), 1603–1638 (2016)
4. Ervin, V.J., Roop, J.P.: Variational solution of fractional advection dispersion equations on bounded domains in  $\mathbb{R}^d$ . *Numer. Methods Partial Differ. Equ.* **23**(2), 256–281 (2007)
5. Gorenflo, R., Mainardi, F., Moretti, D., Pagnini, G., Paradisi, P.: Discrete random walk models for space–time fractional diffusion. *Chem. Phys.* **284**(1), 521–541 (2002)
6. Gorenflo, R., Vivoli, A., Mainardi, F.: Discrete and continuous random walk models for space-time fractional diffusion. *Nonlinear Dyn.* **38**(1–4), 101–116 (2004)
7. Gui, W.-Z., Babuška, I.: The  $h$ ,  $p$  and  $h$ - $p$  versions of the finite element method in 1 dimension. I. The error analysis of the  $p$ -version. *Numer Math.* **49**(6), 577–612 (1986)
8. Gui, W.-Z., Babuška, I.: The  $h$ ,  $p$  and  $h$ - $p$  versions of the finite element method in 1 dimension. II. The error analysis of the  $h$ - and  $h$ - $p$  versions. *Numer Math.* **49**(6), 613–657 (1986)
9. Hilfer, R., Butzer, P.L., Westphal, U., Douglas, J., Schneider, W.R., Zaslavsky, G., Nonnemacher, T., Blumen, A., West, B.: Applications of fractional calculus in physics, volume 128. World Scientific (2000)
10. Jin, B., Lazarov, R., Pasciak, J., Rundell, W.: A finite element method for the fractional Sturm-liouville Problem. arXiv:1307.5114 (2013)
11. Jin, B., Zhou, Z.: A finite element method with singularity reconstruction for fractional boundary value problems. *ESAIM Math. Model. Numer. Anal.* **49**(5), 1261–1283 (2015)
12. Jin, B., Lazarov, R., Zhi, Z.: Petrov-Galerkin finite element method for fractional convection-diffusion equations. *SIAM J. Numer. Anal.* **54**(1), 481–503 (2016)
13. Li, X., Xu, C.: Existence and uniqueness of the weak solution of the space-time fractional diffusion equation and a spectral method approximation. *Commun. Comput. Phys.* **8**(5), 1016–1051 (2010)
14. Liu, Q., Liu, F., Turner, I.W., Anh, V.V.: Approximation of the Lévy-Feller advection-dispersion process by random walk and finite difference method. *J. Comput. Phys.* **222**(1), 57–70 (2007)
15. Mao, Z., Shen, J.: Efficient spectral-Galerkin methods for fractional partial differential equations with variable coefficients. *J. Comput. Phys.* **307**, 243–261 (2016)

16. Mao, Z., Chen, S., Shen, J.: Efficient and accurate spectral method using generalized Jacobi functions for solving Riesz fractional differential equations. *Appl. Numer. Math.* **106**, 165–181 (2016)
17. Metzler, R., Klafter, J.: The random walk's guide to anomalous diffusion: a fractional dynamics approach. *Phys. Rep.* **339**(1), 1–77 (2000)
18. Moffatt, H.K., Zaslavsky, G.M., Comte, P., Tabor, M.: *Topological aspects of the dynamics of fluids and plasmas* (1992)
19. Podlubny, I.: *Fractional differential equations: an introduction to fractional derivatives, fractional differential equations, to methods of their solution and some of their applications*. Academic press, San Diego (1999)
20. Samko, S.G., Kilbas, A.A., Marićev, O.I.: *Fractional Integrals and Derivatives*. Gordon and Breach Science Publication (1993)
21. Shen, J., Tang, T., Wang, L.-L.: *Spectral Methods: Algorithms, Analysis and Applications*. Springer (2011)
22. Yanovsky, V.V., Chechkin, A.V., Schertzer, D., Tur, A.V.: Lévy anomalous diffusion and fractional fokker–planck equation. *Phys. A Stat. Mech. Appl.* **282**(1), 13–34 (2000)
23. Zayernouri, M., Karniadakis, G.E.: Fractional Sturm-Liouville eigen-problems: theory and numerical approximation. *J. Comput. Phys.* **252**, 495–517 (2013)
24. Zayernouri, M., Karniadakis, G.E.: Discontinuous spectral element methods for time- and space-fractional advection equations. *SIAM J. Sci. Comput.* **36**(4), B684–B707 (2014)
25. Zeng, F., Zhang, Z., Karniadakis, G.E.: A generalized spectral collocation method with tunable accuracy for variable-order fractional differential equations. *SIAM J. Sci. Comput.* **37**(6), A2710–A2732 (2015)
26. Zeng, F., Mao, Z., Karniadakis, G.E.: A generalized spectral collocation method with tunable accuracy for fractional differential equations with end-point singularities. To be appeared on *SIAM Journal Science Computer* (2016)
27. Zhao, X., Sun, Z.-Z., Hao, Z.-P.: A fourth-order compact ADI scheme for two-dimensional nonlinear space fractional Schrödinger equation. *SIAM J. Sci. Comput.* **36**(6), A2865–A2886 (2014)